The North Brazil Undercurrent

LOTHAR STRAMMA,* JÜRGEN FISCHER* and JÖRG REPPIN*

Abstract—The flow field in the area of what was thought to be the source region of the North Brazil Current (NBC) off the northeast coast of Brazil between 5°30′S and 10°S was investigated in austral spring during November 1992 and compared with observations in October 1990. The data were taken with several different instruments, including vessel-mounted ADCP, lowered-ADCP, Pegasus, CTD and XBTs. The flow was found off the coast at 5°30′S as well as at 10°S as an undercurrent, the North Brazil Undercurrent (NBUC). The NBUC shows a subsurface core at about 200 m depth with velocities of up to 90.0 cm s^{-1}, resulting in large northward transports of more than 22 Sv in the upper 1000 m. The transport is about the same at 5°30′S and 10°S, hence no net inflow from the east is required to feed the NBUC. The climatological Ekman transport is to the south between 5°30′S and 10°S, and in consequence the northward flow near the surface was reduced and might be one reason for the existence of the undercurrent. The flow near the coast was to the north at 10°S, therefore the Brazil Current had to start as a coastal current south of 10°S. For the zonal sections at 5°30′S and 10°S the geostrophic computations relative to the density surface σ_1 = 32.15 kg m^{-3} (about 1150 m depth) resulted in transports comparable to those obtained from direct measurements. The results further show that the choice of a correct level of no motion can be supported by the direct observations. A shallower reference based on water mass boundaries alone would reduce the NBUC transport to almost zero. Computations with data from the historical data base for austral fall resulted in a weaker NBUC of less than 20 Sv near 10°S, indicating a possible seasonal signal in the NBUC with a stronger NBUC in austral spring.

INTRODUCTION

In the literature there is not much information on the formation region of the North Brazil Current (NBC) south of 5°S. Near the northeast coast of Brazil the South Equatorial Current (SEC) is described as splitting into the southward flowing Brazil Current and the northwestward flowing NBC, as can be seen from the schematic flow field presented by Richardson *et al.* (1994). Stramma *et al.* (1990) described near 15°S a northwestward flow of 8 Sv (1 Sverdrup = 10^6 m^3 s^{-1}) crossing 30°W. In February and March the southern part of the SEC reaches the shelf near 10°S, and about 4 Sv continues towards the northwest into the NBC. Another branch, is also carrying 4 Sv, turns southward as the beginning of the Brazil Current. At 30°W another westward flow of approximately 8–10 Sv enters the area near 10°S and not only strengthens the NBC (Stramma *et al.*, 1990) but also contributes to the South Equatorial Countercurrent (SECC), which is sometimes observed between 7°S and 9°S (Molinari, 1983). A second eastward flowing current band observed south of the equator is the South Equatorial Undercurrent (SEUC) at about 3°S

---

*Institut für Meereskunde an der Universität Kiel, Düsternbrooker Weg 20, 24105 Kiel, Germany.

to 5°S (Molinari, 1982). The transport distribution (Stramma *et al.*, 1990) near 10°S was based on data from February and March, and, as will be shown later, the reference level used was probably not the best choice.

Surface drifters drogued at 15 m depth deployed during *Meteor* cruise 14 in October 1990 at about 33°W between 6°S and 9°S all turned to the south near the coast (W. Krauss, pers. comm.). Ship drift data have long shown the Brazil Current originating in the bifurcation of the SEC near Cabo de Sao Roque (5°30'S) (Rennell, 1832), a feature that also can be seen in the trajectories of satellite-tracked drifting buoys (Molinari, 1983; Reverdin and McPhaden, 1986). However, the initial southward drift near Cabo de Sao Roque is probably only the Ekman layer, which has the same southward motion (Richardson and Walsh, 1986; Arnault, 1987) observed by the drifters; there seems to be no southward geostrophic surface current north of 10°S (Arnault, 1987), although Reid's (1989) map of adjusted steric height at 0 db showed a southward flow at the Brazilian coast at 9°S, while the southward component for the adjusted steric height of 250 db was located south of 20°S (Reid, 1989; Reid, 1994).

Until now, few details have been known about the source region of the NBC or about possible seasonal signals in the flow field, Data from different instruments on two cruises with R.V. *Meteor*, in October 1990 and November 1992, are used here (a) to investigate whether the splitting of the SEC happens north of 10°S in austral spring, (b) to describe, from closed boxes, the transports in the "source region of the North Brazil Current" and (c) to look for indications of a seasonal signal by comparing the transports at 5°30'S and 10°S with the transports of sections from the historical data base and a section at 5°30'S done by R.V. *Meteor* in June 1991.

THE DATA

The cruise tracks and CTD station locations between 5°S and 10°S east of the Brazilian coast from *Meteor* cruise M14-2 (October 1990) and *Meteor* cruise M22-2 (November 1992) are shown in Fig. 1. Although the sections from both cruises at around 5°S are located between 5°30'S and 5°00'S, in the following text the sections are referred to as being 5°30'S as the strong current band was crossed at 5°30'S. For a comparison at 5°30'S another section at 5°30'S is available from *Meteor* cruise M16-3 in June 1991.

In October 1990 10 CTD stations were made at 5°30'S between the coast and 32°32'W. For the box along about 33°W and 9°30'S (in the following referred to as 9°S) no time for CTD stations was left. Along these two sections in total 25 XBTs were deployed. The vessel-mounted ADCP (VM-ADCP) operated along all three sections and collected the velocity distribution for the upper 0 to 180–200 m. An ADCP was mounted to the CTD-rosette and lowered with the CTD (in the following named lADCP) to measure a continuous velocity profile. In 1990 only three lADCP profiles were obtained near the coast at 5°30'S.

In November 1992 the lADCP worked on all CTD stations of the box except for two stations in the center of the 5°30'S section. At 5°30'S eight Pegasus profiles were made between the shelf and 31°30'W. In total 15 CTD stations were made along 5°30'S between the coast and 30°W, four stations between the 5°30'S and 10°S section and 10 stations along the 10°S section between the coast and 32°30'W (Fig. 1). Along the entire box the VM-ADCP sampled the upper ocean velocity data. The VM-ADCP was installed in the hydrographic well, and the measurement range varied between 270 and 400 m depth.
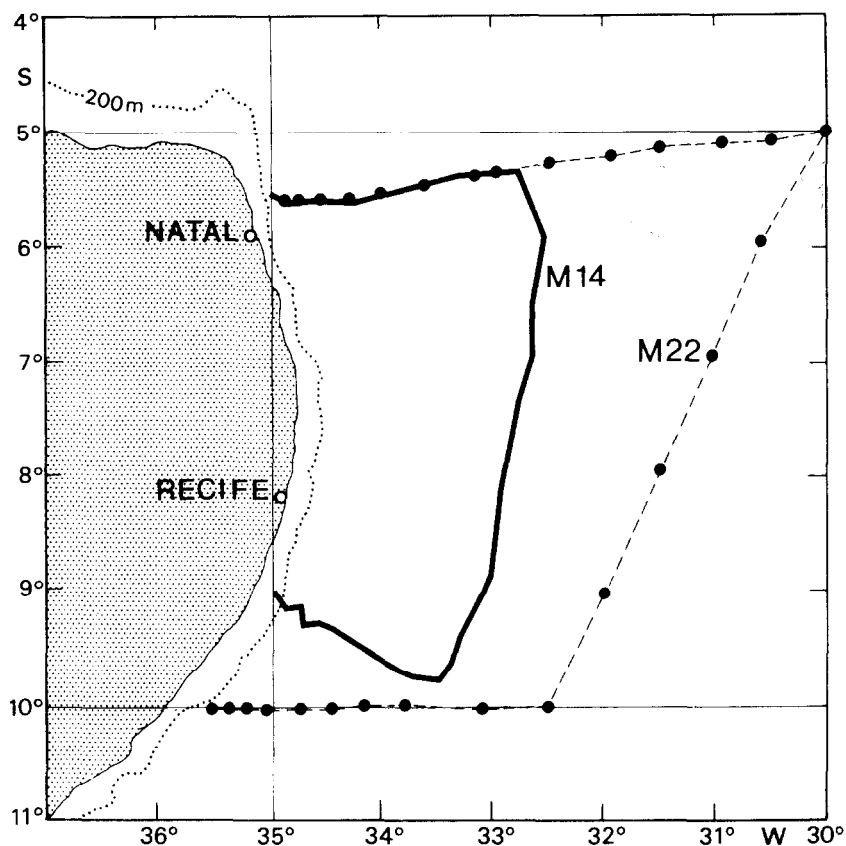
Fig. 1. Cruise tracks (lines) with VM-ADCP measurements off the northeast coast of Brazil for *Meteor* cruise M14-2 (M14) in October 1990 and M22-2 (M22) in November 1992 with station locations as dots. Included is the 200 m depth contour.

METHODS

During *Meteor* cruise M14 in October 1990, a self-contained ADCP mounted in the hydrographic well had to be used because of defective transducers in the built-in vessel-mounted ADCP. External heading and navigation from the ship's central data recording system were used to correct the averaged profiles for heading and speed over ground. Due to the lower source level of the self-contained 150 kHz ADCP compared with a normal VM-ADCP, the measurement range was restricted to the upper 180–200 m depth. The data were calibrated with respect to the alignment angle of the transducers and interpolated to a regular grid of 10 m vertically and $0.1°(10$ km) horizontally using a Gaussian weighting function with a cut-off radius of 20 m and $0.2°$, respectively. During the cruise in November 1992 (M22), a 150 kHz VM-ADCP was used. The measurement range varied between 270 m and 400 m depth depending on the amount of scatterers in the upper ocean. Unfortunately a defect in one synchro-converter led to course dependent heading offsets of up to 10 degrees. However, within the ensemble interval (5 min) the heading variations were small, and it was therefore possible to correct the 5 min averages with external heading measurements. Periods with heading variations larger than a few degrees were

omitted; these occurred during the deceleration and acceleration phases before and after each station. After this correction the same calibration and interpolation procedure as for M14 was applied. Remaining uncertainties due to the heading and GPS errors together with the short time inaccuracies of the ADCP were estimated to be of up to 10 cm s^{-1}. But since these errors are mostly random, they will be reduced when integrating over many ensembles. By the regridding procedure, i.e. smoothing over about 20 km, corresponding to 12 ensembles, the error of the interpolated data was reduced to 3 cm s^{-1}. For transport calculations, e.g. over the width (100 km) of the North Brazil Undercurrent (NBUC) and 250 m depth, the uncertainty was estimated to be less than ±1 Sv. As the VM-ADCP does not resolve the upper few meters of the ocean, the shears were extrapolated from the uppermost two bins to the surface for velocity and transport calculations.

In addition to the VM-ADCP, direct observations of the deeper velocity field were obtained by an acoustic dropsonde, the Pegasus (Spain *et al.*, 1981), which was used on several stations along 5°30'S, and by lowering an ADCP (lADCP) with the CTD (Fischer and Visbeck, 1993). Both methods compare reasonably well, and the estimated errors of the lADCP (order 5 cm s^{-1}) are a little larger than those of Pegasus profiles (Send, 1994).

The lADCP was exchanged due to a broken transducer at the 5°30'S section in November 1992, and the new "broad-band" ADCP was an untested device which showed large data gaps on the upward casts, but only during casts which exceeded 2000 m. However, the downward casts could be used on those stations to determine relative velocity profiles which were then referenced by the VM-ADCP on the same station by minimizing the mean between the lADCP and VM-ADCP velocity differences in the depth range 50–250 m. This was done for all stations west of 34°W or the 5°30'S section and all stations along 10°S.

Based on the assumption that the flow field was resolved by the station grid (which was not the case on the diagonal section between 5°S and 10°S), and that the lADCP errors of 5 cm s^{-1} were random from station to station, the estimated transport uncertainty for the six stations across the 1000 m deep North Brazil Undercurrent would be of the order of ±2 Sv.

The calibration of the CTD data resulted in accuracies of 0.002°C in temperature, 0.003 in salinity and 3 dbar in pressure. The CTD data were used to calculate geostrophic velocities and transports. For geostrophic computations a reference depth is needed to convert from relative to absolute velocities. Based on an investigation of the water mass distribution and the knowledge of the spreading directions of the different water masses, Stramma (1991) used a reference depth of $\sigma_1 = 32.15$ kg m^{-3} for an investigation of the SEC in the Atlantic. This density layer is located at a depth of about 1150 m and represents the boundary between the bottom of the northward flowing upper branch of Circumpolar Deep Water and the top of the southward flow of Upper North Atlantic Deep Water. In the following the density $\sigma_1 = 32.15$ kg m^{-3} was used as the reference depth for the geostrophic calculations.

The depth of the 1.8°C potential temperature was described by Molinari *et al.* (1992) as the lower boundary of the deeper NADW layer. This isotherm could be another possible reference level for geostrophic computations (Rhein *et al.*, 1995). The 1.8°C isotherm was found between 3680 m depth near the South American continent and 3900 m further offshore. It indicates the boundary between the lower North Atlantic Deep Water (lNADW) and the Antarctic Bottom Water (AABW) and coincides roughly with the density surface $\sigma_4 = 45.90$ kg m^{-3}. As this density surface is far away from the layer investigated, we prefer to use the reference level closer to the investigated layer. As will be

shown later, the deeper reference level led to differences in the details of the geostrophic current fields compared to the direct observations, while currents calculated relative to the density $\sigma_1 = 32.15$ kg m^{-3} compare much better with the direct velocity observations.

SECTION AT 5°S

Vessel-mounted ADCP

The velocity distribution in the upper ocean from the VM-ADCP in November 1992 is presented in Fig. 2a–d. The northward velocity component at 5°30'S (Fig. 2a) shows that the flow was located near the coast with velocities exceeding 80 cm s^{-1}. The core of current is found around 200 m depth with most of the current sheared away towards the surface; thus the flow field has the structure of an undercurrent, the North Brazil Undercurrent. The zonal component near the coast at 5°30'S showed only weak westward velocities of 10 cm s^{-1} in 100–200 m depth due to the nearly meridional shelf (therefore not shown). While the NBUC reached its maximum speed at 200 m depth, the velocity at the sea surface was reduced to about 20 cm s^{-1} northward. The major northward flow of the NBUC was found west of 34°W, while between 31°W and 34°W only weak southward velocities were observed. An eastward extension of the NBUC was observed at about 150 m depth. It appeared as a 70 km long and only about 100 m thick velocity tongue with more than 10 cm s^{-1}. In October 1990 the VM-ADCP section at 5°30'S (Fig. 3a) also showed a northward subsurface-current maximum of more than 90 cm s^{-1}, and as was the structure found in November 1992, the eastward extending velocity tongue was found at about 150 m depth. Due to the limited vertical range (200 m), the core of the NBUC was not completely resolved.

Lowered ADCP

The deeper reaching flow in November 1992 (surface to 1200 m depth) was measured by the lADCP (Fig. 4a). For the upper layer (0–250 m) this data set compared well with the VM-ADCP velocities (Fig. 2a). East of 34°W the lADCP data were adjusted to the VM-ADCP and an independent comparison was not possible. Below the current core at 200 m depth the currents were sheared to 40 cm s^{-1} near 500 m, and with weaker shears below 500 m the NBUC was still visible in 1000 m depth. Between 31°W and 34°W weak southward flow of 10 cm s^{-1} or less was observed, and between 30°W and 31°W a fairly deep reaching band of northward flow of up to 20 cm s^{-1} was found in November 1992.

Geostrophic calculations

Geostrophic velocities for November 1992 (M22) were calculated relative to the depth of the isopycnal $\sigma_1 = 32.15$ kg m^{-3} which varies between 1130 m and 1190 m (Fig. 4b). The general structure of the geostrophic flow field (Fig. 4b) is quite similar to the direct current observations with respect to amplitude and extent of the NBUC. However, the geostrophic velocity field showed higher variability in the upper 100 m of the ocean. East of the NBUC southward flow is found between 400 m and 1100 m with velocities up to 10 cm s^{-1}, which is also present but a little weaker in the lADCP data. On the eastern side of the section between 30°W and 31°W, northward flow is found in both representations, but more intense in the lADCP data between the surface and 800 m depth.
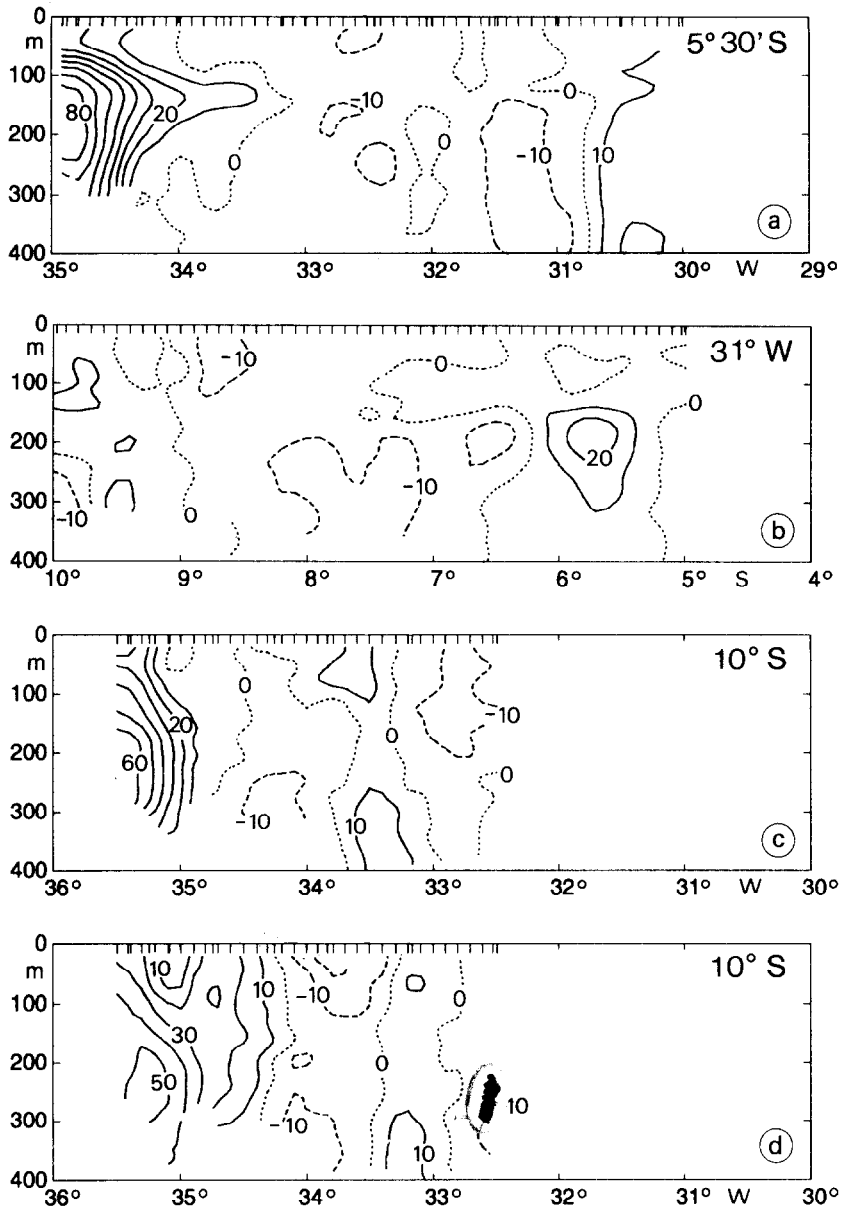
Fig. 2. VM-ADCP velocity in cm s^{-1} in November 1992 for (a) the northward component at 5°30'S, (b) perpendicular to the cruise track at 31°W (positive northwestward), (c) the eastward component at 10°S and (d) the northward component at 10°S. The zero velocity is dotted; negative values are dashed lines with 10 cm s^{-1} contour intervals.

For October 1990 the structure of the geostrophic velocity field relative to $\sigma_1 = 32.15$ kg m^{-3} at 5°30'S (Fig. 4c) is comparable to the velocity distribution in November 1992. As in November 1992 a southward flow at about 300–1100 m was observed in October 1990. The northward flowing NBUC with a subsurface velocity maximum was again found near the
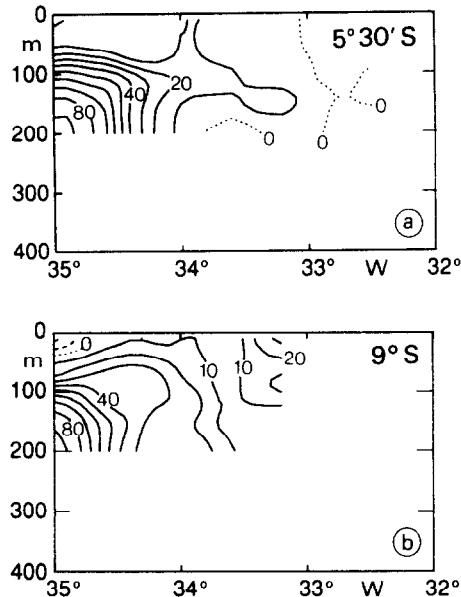
Fig. 3.   VM-ADCP velocity in cm s^{-1} in October 1990 for northward component at (a) 5°30'S and (b) 9°S.

coast. The northward transport in the upper ocean was found west of 33°30'W in October 1990 and the highest velocities of the NBUC were observed west of 34°15'W. One CTD station was omitted which led to a maximum velocity at 200 m of 180 cm s^{-1}, probably caused by the short station spacing of 10 km for the station pair. One of the three lADCP profiles taken in the NBUC region showed maximum velocities of 100 cm s^{-1} at 180–300 m in October 1990, while the VM-ADCP showed maximum velocities of 90 cm s^{-1} at 180 m depth (Fig. 3a). The geostrophic velocity without the omitted profile (Fig. 4c) showed a value of 100 cm s^{-1} in the core of the NBUC and therefore agreed with the direct measurements. As the eliminated station was not an end-point of the section, the one profile in question has no influence on the transport computations.

Table 1(a) shows the geostrophic transport at 5°30'S for the layers across the entire section in October 1990 and November 1992. The total section transports are quite similar for both cruises. To investigate the geostrophic transports of the western boundary current off the coast, the transports from the coast to the location where a flow reversal appeared were calculated for October 1990 and November 1992 (Table 1(a)). The northward transport at 5°30'S in October 1990 summed up to 31.9 Sv and in November 1992 to 24.2 Sv in the upper 1000 m. With the deeper reference $\sigma_4 = 45.90$ kg m^{-3}, transports out to flow reversal were reduced to 28.9 Sv; i.e. there is a 4 Sv uncertainty in using different reference levels. In October 1990 the NBUC transport was larger than in November 1992, but a stronger southward component east of the NBUC led to the similar transports for the entire section in both cruises.

DIAGONAL SECTION AT 31°W

The westward flow across 31°W from VM-ADCP was quite weak in November 1992. The flow perpendicular to the ship section (Fig. 2b) was northwestward between 5°S and
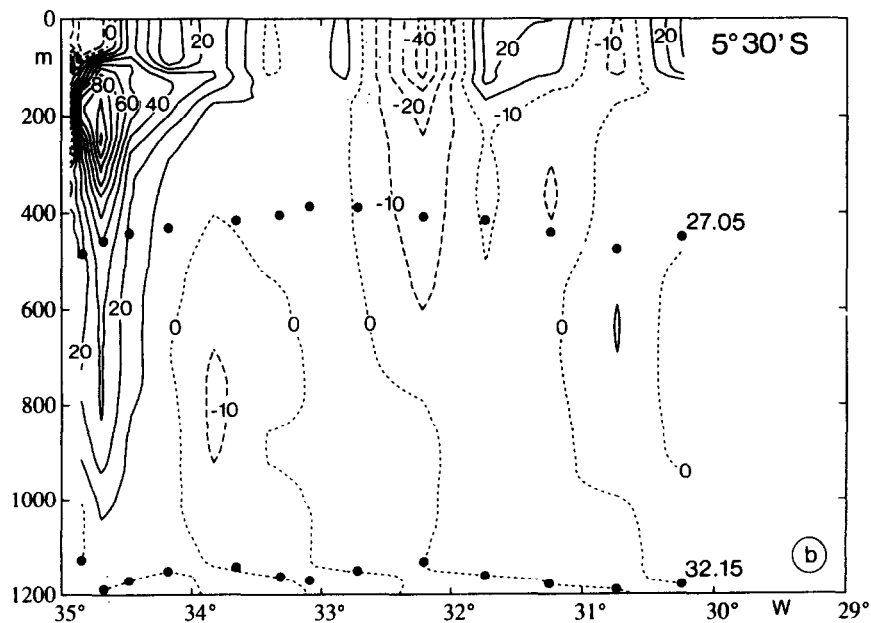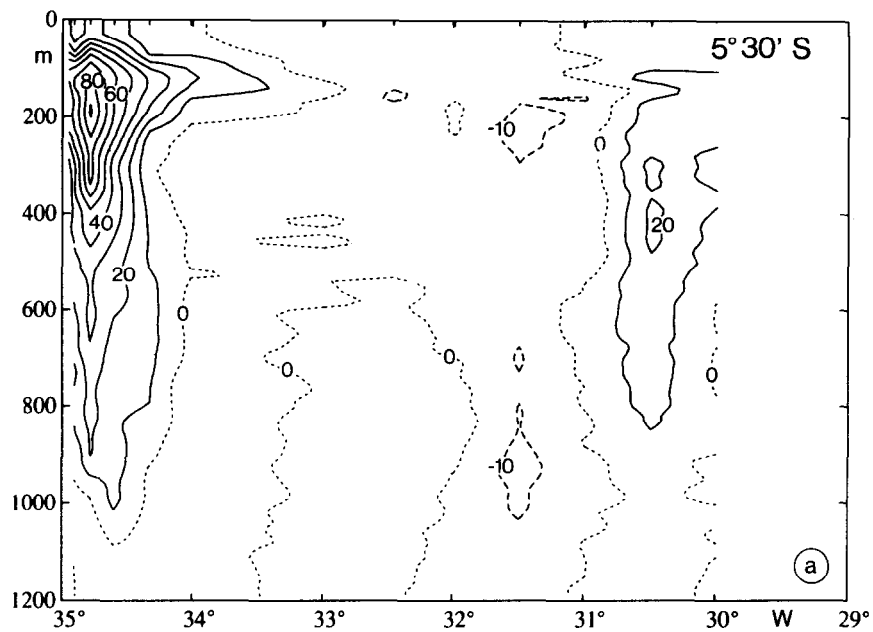
Fig. 4.   Velocity in cm s^{-1} for the northward component at 5°30′S for (a) lowered-ADCP in November 1992, (b) geostrophic velocity relative to $\sigma_1 = 32.15$ kg m^{-3} in November 1992 and (c) geostrophic velocity relative to $\sigma_1 = 32.15$ kg m^{-3} in October 1990. The depths of the densities $\sigma_0 = 27.05$ kg m^{-3} and $\sigma_1 = 32.15$ kg m^{-3} are included as dots in (b).
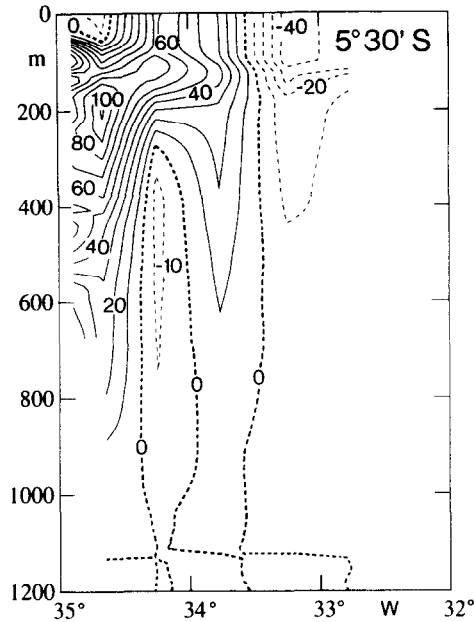
Fig. 4. (*Continued*)

Table 1. *Geostrophic transports at (a) about 5°30′S relative to* $\sigma_1 = 32.15$ kg m^{-3}. *Positive transport is to the north. The total and near coast transport at 10°S is given in (b). The flow reversal is the location where the velocity field changed the flow direction. For comparison the lADCP transport out to the longitude of the flow reversal is shown in the last column*

| (a) 5°30′S | Entire section | | Coast to reversal | | |
| | Oct. 90 between 34°56′ and 32°32′W | Nov. 92 between 34°57′ and 30°00′W | Oct. 90 between 34°56′ and 33°30′W | Nov. 92 between 34°57′ and 32°27′W | Nov. 92 lADCP to flow-reversal |
Depth layer					
0–100 m	1.2	3.8	5.5	2.9	1.7
0–250 m	9.9	12.0	17.2	12.3	7.8
0–500 m	17.1	17.0	27.0	19.3	12.7
0–1000 m	19.1	20.2	31.9	24.2	16.7

| (b) 10°S | Nov. 92 between 35°30′ and 32°30′W | Nov. 92 between 35°30′ and 34°15′W | Nov. 92 lADCP to flow-reversal |
Depth layer			
0–100 m	1.9	2.5	2.7
0–250 m	7.9	8.3	8.6
0–500 m	14.9	16.0	16.5
0–1000 m	19.9	22.2	23.5

6°30'S and south of 9°S. Maximum speeds were up to 20 cm s^{-1} at 200 m depth. Between 6°30'S and 9°S there was a weak southeastward flow, balancing the total VM-ADCP transport across the section to almost zero. The southeastward flow near 8°S is found where the SECC should be located, and the eastward flow could be the signature of this current.

In October 1990 the diagonal section closing the box was located at about 33°W (Fig. 1). The VM-ADCP showed between 5°30'S and 8°30'S a southwestward flow and between 8°30'S and 9°40'S a southeastward flow in the upper 200 m. This flow structure led to a net westward transport of 4.2 Sv.

THE 9°S AND 10°S SECTIONS

Vessel-mounted ADCP

The velocity distribution at 10°S from the VM-ADCP in November 1992 showed the largest velocities near the coast in both the eastward and northward component (Fig. 2c and d) with velocities of about 60 cm s^{-1}. At this latitude the Brazilian shelf (200 m isobath) is oriented toward about 35°T (Fig. 1), and the NBUC followed the topography in the northeastward direction. Alongshore speeds associated with the NBUC showed velocities of up to 90 cm s^{-1} similar to what was found farther north. Another similarity between the two sections was the subsurface velocity core at about 200 m depth with weaker northeastward velocities closer to the sea surface. The strong flow was again restricted to the coast while to the east of the NBUC the currents were weak.

The VM-ADCP section at 9°S in October 1990 (Fig. 3) showed a northward subsurface-current maximum of more than 90 cm s^{-1} below 150 m depth. Towards the surface the current was sheared away to less than 10 cm s^{-1}; at the westernmost part of the 9°S section there was even a southward flow very close to the surface. Horizontally, the NBUC current core extended to about 34°W, corresponding to about 100 km width. Northward transports of the top 200 m out to 34°W were similar for the 5°30'S and 9°S sections, 6.9 Sv at 5°30'S and 7.4 Sv at 9°S. The 0.5 Sv imbalance is within the error bounds. Out to 33°06'W (easternmost longitude of the 9°S section) the transports were 9.8 Sv at 9°S and 8.4 Sv at 5°30'S. At the 9°S section the zonal velocity component was small; eastward velocities of 10 cm s^{-1} were found only near the core of the NBUC (east of 34°30'W). Further offshore zonal currents were even smaller. Compared to the sections at 10°S in November 1992, where both velocity components contributed about equally, the flow at 9°S was predominantly northward, following the topography at this latitude (Fig. 1). Therefore, the NBUC appears to turn from a northeastward direction at 10°S to a northward direction at 9°S, continuing northward to 5°30'S.

Lowered ADCP

For better comparison of the flow structure at 5°30'S and 10°S the lADCP currents at 10°S were rotated (by 35°) according to the orientation of the topography, and the along-shore components for both sections in November 1992 are shown versus offshore distance (Fig. 5). At both latitudes a subsurface core was observed in about 200 m depth with maximum velocities of 90 cm s^{-1} at 5°30'S and 80 cm s^{-1} at 10°S. At 10°S the NBUC appeared to extend deeper, with the 10 cm s^{-1} isotach reaching almost 1100 m depth.
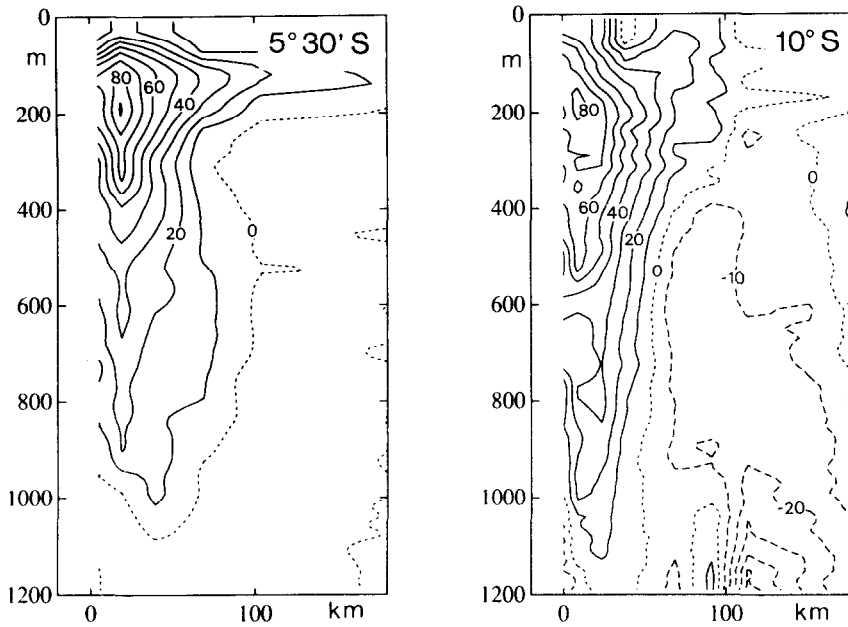
Fig. 5.   The North Brazil Undercurrent velocity distribution versus offshelf distance (isolines for 10 cm s^{-1} contour intervals) at 5°30'S and 10°S in November 1992 from the lowered-ADCP rotated to show the along-shore component.

There was no indication of an eastward extension of the velocity core near 150–200 m which seemed to be a permanent feature of the flow structure at 5°30'S (Fig. 5).

Geostrophic calculations

Geostrophic transports relative to σ_1 = 32.15 kg m^{-3} (Table 1b) show that at 10°S the western boundary current transported 22.2 Sv northward in the upper 1000 m west of the flow reversal. Compared with the transport at 5°30'S, 92% of the geostrophic transport of the NBUC in November 1992 crossed 10°S, and only a small net contribution of 2 Sv (within the error margins) was needed to balance the transports between 10°S and 5°30'S. Such a small contribution could be explained by the unresolved flow on the shallow shelf or could be an inflow from the east.

Plots of geostrophic transport versus offshore distance during *Meteor* cruise 22 show that there were close similarities between the two latitudes from the coast out to the offshore edge of the NBUC. On the offshore side of the NBUC the differences were a little larger, presumably due to the one station at 5°30'S that led to a singular transport maximum. Summarizing, the NBUC in November 1992 occurred as a strong subsurface boundary current flowing along the edge of the Brazilian shelf in the latitude range 10°S—5°30'S without a larger contribution from the east in that latitude belt. Of the total transport (0–1000 m) 40–50% was attributed to the top 250 m and 70–80% to the top 500 m (Table 1). Therefore, the major transport took place in the upper 500 m, with a tendency of slightly larger transport fraction in the upper ocean at 5°30'S. On both sections we observed a reversal of the flow field at the offshore edge of the NBUC (Figs 6,7). The transport
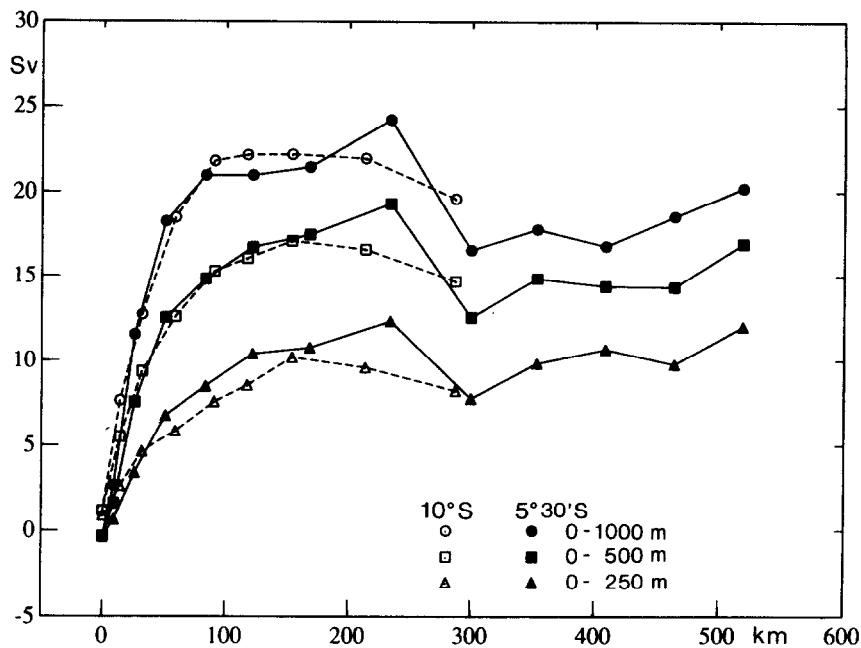
Fig. 6. Cumulative geostrophic northward transport relative to $\sigma_1 = 32.15$ kg m^{-3} in Sv in November 1992 at 5°30'S (solid symbols) and 10°S (open symbols) for the layers 0–250 m (triangles) 0–500 m (squares) and 0–1000 m (dots) plotted versus offshelf distance.

associated with this counter flow was about 2 Sv (0–1000 m); from the edge of the NBUC out to 300 km offshore the continental shelf.

During *Meteor* cruise 14 in October 1990 two XBT (760 m deep) sections were made south of 5°S, at about 33°W and at about 9°S (Fig. 1), as no time was available for CTD casts. Geostrophic transport estimates were attempted from these two sections using salinities of the Levitus (1982) summer data set (August, September, October) from two neighbouring 1 × 1 degree squares in combination with the measured XBT temperatures. The geostrophic computation was made relative to 700 m depth, the largest depth possible. The velocities from the XBTs with Levitus salinities led to a velocity field which was not comparable to the velocity distribution from the VM-ADCP. It had to be concluded that a combination of XBTs (reaching 760 m) and Levitus salinities is not usable to investigate the velocities and transports in the horizontally variable region of the NBUC without any further adjustments.

BOX TRANSPORTS

Plots of the mean velocity field (Fig. 7a,b) illustrate the characteristic structures of the NBUC: the intense currents following the 200 m depth contour (Fig. 7b) and the reduced current amplitude in the near surface layer (Fig. 7a). It is interesting to note that the flow at 10°S turned northward with increasing distance from the topography, leading to a convergent flow. In the upper 50 m at 32°W, between 8°S and 9°S, the flow was to the east. This is the region where the SECC should be located, and the eastward flow could be the signature of this current. On the diagonal section between 5°S and 6°30'S at 150–200 m
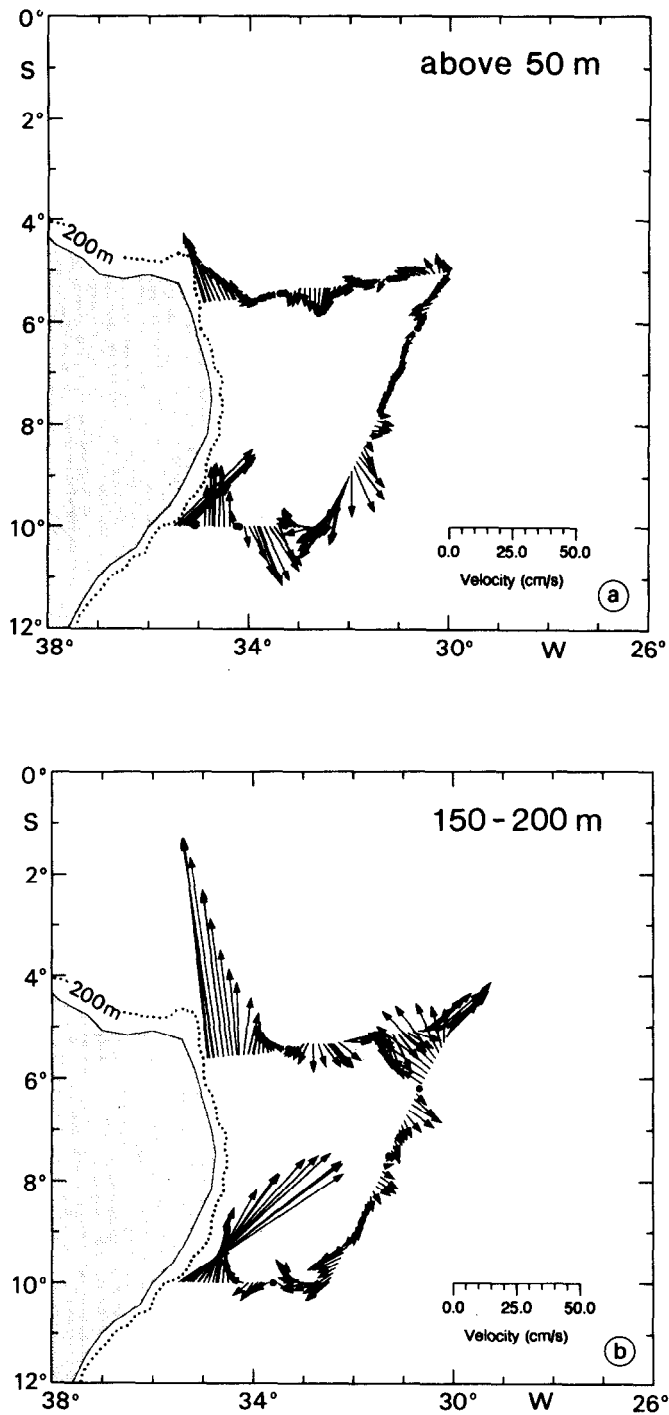
Fig. 7.   Mean velocity for the layers (a) above 50 m and (b) 150–200 m with the same scale in velocity arrows in November 1992 from VM-ADCP data smoothed by a Gaussian weighting function. Included are the 200 m depth contours.

depth, the flow was to the northwest and at the eastern end of the 5°30'S section it was to the northeast. This might be a contribution from the SECC to the South Equatorial Undercurrent (SEUC), normally found between 3°S and 5°S. Subsurface velocity enhancement (Fig. 7) supports the interpretation that this might be some contribution to the SEUC.

Transport budgets for the entire box in November 1992 were calculated by using VM-ADCP, lADCP and geostrophy relative to $\sigma_1 = 32.15$ kg m^{-3} (Table 2). The transports 0–100 m and 0–250 m of the VM-ADCP and the lADCP agree well for the zonal sections at 5°30'S and 10°S, but in part this is caused by the fact that the lADCP was adjusted to the VM-ADCP for all stations west of 34°W at the 5°30'S section and all stations along 10°S. At 31°W no lADCP transport is given, as the station spacing of about 120 km is too large to estimate reliable transports from the single point profiles without any information on the flow field in between. No correlation was found between neighbouring stations except that all of the profiles showed weak currents in the depth layer 400–700 m. Information on the flow field between the stations is contained only in the density signature used for geostrophic computations. On the other hand, the use of a reference depth chosen from the general water mass distribution did not always fit the zero velocity found in direct

Table 2. VM-ADCP, lowered-ADCP, geostrophic (relative to $\sigma_1 = 32.15$ kg m^{-3} with Ekman component in brackets) geostrophic plus Ekman, and adjusted geostrophic transports (to the directly measured 1000–1100 m velocities at 5°30'S and 400–700 m at 31°W) at (a) about 5°30'S, (b) about 31°W and (c) 10°S in November 1992 for the entire sections. Positive transport is into the box (south at 5°30'S, northwest at 31°W and north at 10°S)

Depth layer	VM-ADCP	Lowered-ADCP	Geostrophy (Ekman)	Geostrophy plus Ekman	Adjusted geostrophy
(a) 5°30'S					
0–100 m	−1.4	−1.5	−3.8 (3.0)	−0.8	−4.0
0–250 m	−7.9	−8.4	−12.0 (3.0)	−9.0	−12.6
0–500 m	—	−12.8	−17.0 (3.0)	−14.0	−18.1
0–1000 m	—	−19.6	−20.2 (3.0)	−17.2	−22.5
(b) 31°W					
0–100 m	−0.7	*	3.5 (0.1)	3.6	3.0
0–250 m	0.0	*	6.9 (0.1)	7.0	5.0
0–500 m	—	*	6.8 (0.1)	6.9	3.1
0–1000 m	—	*	6.6 (0.1)	6.7	−0.9
(c) 10°S					
0–100 m	1.5	1.6	1.9 (−0.7)	1.2	†
0–250 m	7.2	7.4	7.9 (−0.7)	7.2	†
0–500 m	—	16.8	14.9 (−0.7)	14.2	†
0–1000 m	—	(23.8‡)	19.9 (−0.7)	19.2	†
(d) total box					
0–100 m	−0.6	—	1.6 (2.4)	4.0	—
0–250 m	−0.7	—	2.8 (2.4)	5.2	—
0–500 m	—	—	4.7 (2.4)	7.1	—
0–1000 m	—	—	6.3 (2.4)	8.7	—

*Station spacing of 120 km too large to estimate reliable transports.

†lADCP showed too large velocities below 500 m on eastern side, no adjustment possible.

‡Below 500 m from coastal profile to flow reversal.

velocity estimates from the IADCP. The major difference is a geostrophic inflow of 6.9 Sv from the east across 31°W in the upper 250 m, while the deeper layers have no net contribution in the geostrophic calculations. Along the same section the VM-ADCP transports show no net inflow in the upper 250 m.

Another significant difference between geostrophic and direct current measurement transports is evident for the upper layers, 0–100 m depth and 0–250 m depth, at 5°30'S. There, the transport values from the VM-ADCP and the IADCP are smaller than the geostrophic transports (Fig. 8a). The same is true of the 10°S section in November 1992 (Fig. 8b), with somewhat smaller differences compared to the 5°30'S section.

For the entire box the imbalance in the upper 250 m is 0.7 Sv outflow from the VM-ADCP measurements and 2.8 Sv inflow from the geostrophic computations. This imbalance is surprisingly low considering that the survey was completed within seven days and might therefore have been non-synoptic. The box is also not completely closed and some water might escape between the coast and the western end of the zonal sections. For the deeper layer the imbalance can be computed only for the geostrophic transport. The imbalance in the geostrophy for the upper 1000 m is an inflow of 6.3 Sv without adjustment to the ADCP and if the Ekman component is not taken into account.

The upper layer transports for October 1990 (Table 3) were based on VM-ADCP measurements and geostrophy relative to $\sigma_1 = 32.15$ kg m^{-3} (only at 5°30'S). The transport for the 0–100 m depth layer is composed of 1.1 Sv entering the box from the east across 33°W, 1.8 Sv leaving the box across 5°30'S, and 3.8 Sv entering across 9°S. This leads to the imbalance of 3.1 Sv inflow for the upper 100 m of the box. In the upper 200 m, 4.2 Sv enter the box from the east across 33°W and from the south with 10.7 Sv across 9°S. An outflow of 8.1 Sv left the box to the north across 5°30'S and the resulting imbalance of the box transport was an inflow of 6.8 Sv. The transport uncertainty was estimated to be of the order of 3 Sv for the upper 200 m being a factor of 2 smaller than the imbalance. At 5°30'S the transport estimate from the VM-ADCP compares well with the geostrophic transport (Table 3). It remains an open question regarding what causes the large transport imbalance. One reason might be that the measurements of the box extended over 4.5 days and were therefore non-synoptic. Another reason of course might be the Ekman flow, with the question whether the horizontal transport balance has to be zero in a region where there is a large Ekman convergence and associated downwelling. The choice of depth layers instead of isopycnals as transport boundaries might lead to imbalances. Onshelf flow was not measured and it could possibly contribute as well.

EKMAN LAYER

A large part of the differences between the direct transports and the geostrophic transports can be explained by the Ekman transport. This flow component is included in the direct measurements but not in the geostrophic transports. Ekman transports across the three sections of the box were calculated after Stramma and Isemer (1988) using the pseudo-windstress values of the area (Servain and Lukas, 1991). From this data set mean November stresses averaged over the years 1985–1989 were available on a 2° × 2° grid. The resulting Ekman transports (Table 2, in brackets) are 3.0 Sv to the south across the entire 5°30'S-section, 0.7 Sv to the south across the 10°S section and negligible transport (0.1 Sv) perpendicular to the diagonal section at about 31°W, because the latter is oriented along the direction of the Ekman flow.

The combined geostrophic and Ekman transport compares well with the direct current observations. The remaining difference at 5°30'S of 1 Sv is well within the accuracy bound of ±2 Sv. At 10°S the combined geostrophic and Ekman transports were in agreement (less than 0.2 Sv difference) with the direct estimates of the upper 250 m. How much of the observed differences might be attributed to variability of the Ekman transport was estimated from actual ship winds. The Ekman transport across 5°30'S is 2.2 Sv compared to 3.0 Sv from the monthly mean winds and across 10°S 1.1 Sv southward compared to 0.7
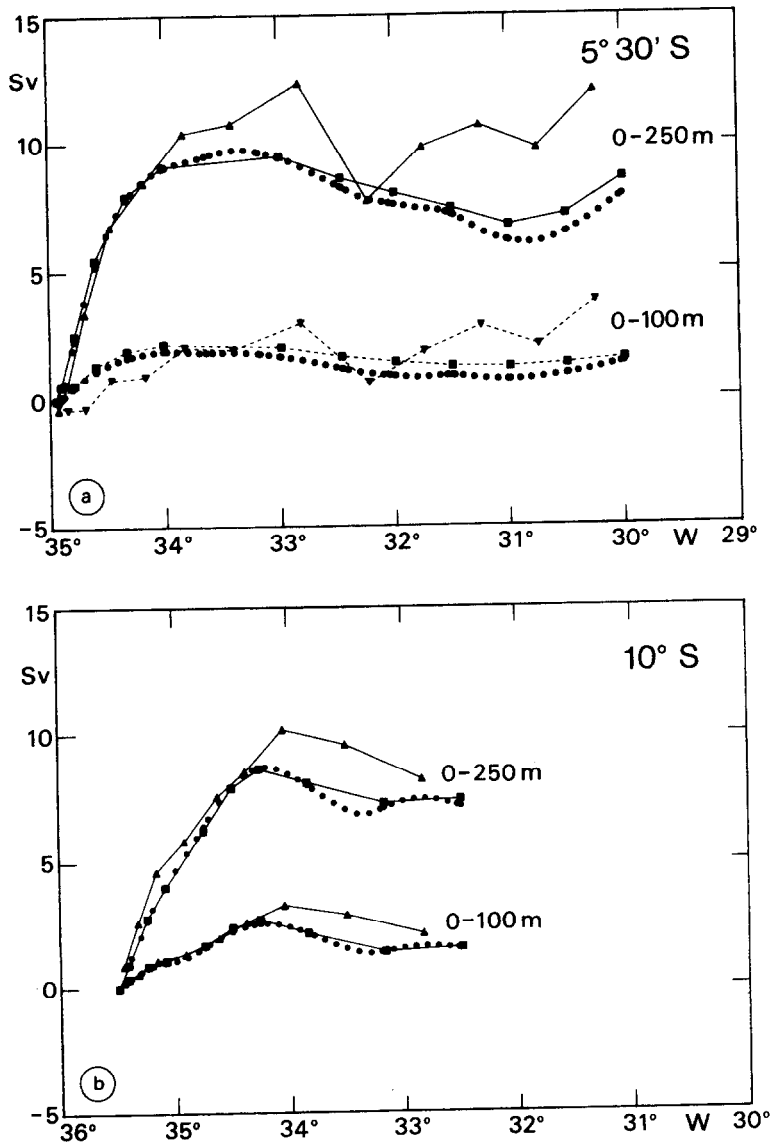

Fig. 8. Cumulative northward transport in Sv at (a) 5°30'S and (b) 10°S in November 1992 for the layer 0–100 m and 0–250 m for VM-ADCP (dots), IADCP (squares) and geostrophic transport relative to $\sigma_1 = 32.15$ kg m^{-3} (triangles).

Sv from the mean wind field. Therefore, a variability of about 1 Sv is possible just from variability in the wind data taken to compute the Ekman transport.

METHOD COMPARISON

From the direct current observations close to the continental shelf at $5°30'S$ (Fig. 4) a level of no motion is hard to detect, but a layer of low vertical shear and small horizontal variability is found roughly between 1000 m and 1100 m. Combined Pegasus and lADCP-velocities averaged over this layer (Fig. 9a) vary by ± 9 cm s^{-1} following a smooth wavelike structure with about 200 km wavelength. A reference velocity was then determined for the mean position of each geostrophic station pair by fitting a cubic spline through the direct observations. Where Pegasus stations were available the Pegasus velocities were used; otherwise the lADCP velocities were used. An immediate result (Fig. 9a) is that the geostrophic velocities with the reference level of $\sigma_1 = 32.15$ kg m^{-3} compare much better to the direct velocities than the velocities relative to density $\sigma_4 = 45.90$ kg m^{-3}. The latter was found to be a good reference for the deep circulation (Rhein et al., 1994). In addition the mean velocity of the entire upper ocean from 10 m to 1000 m is presented (Fig. 9b). This figure clearly shows the influence of the NBUC on the mean velocity and the good agreement between the direct measurements and geostrophic calculations relative to $\sigma_1 = 32.15$ kg m^{-3}.

Adjusting the geostrophic currents to mean speeds in the 1000–1100 m layer (see above) results in a strong similarity of the NBUC in magnitude and horizontal dimension between direct and geostrophic currents. Core velocities of more that 80 cm s^{-1} are found again below the 150 m depth at which the current extends out to $33°30'W$. Below that depth the width of the current decreases, with a weak return flow at its eastern flank. Obvious differences between the two measurements exist in the top 100 m where the geostrophic shear almost vanishes, whereas the directly measured currents show stronger shear. This difference could be due to the absence of the Ekman velocities in the geostrophic

Table 3. *VM-ADCP and geostrophic (relative to $\sigma_1 = 32.15$ kg m^{-3} at 5°30'S) transports at (a) about 5°30'S, (b) about 33°W and (c) 9°S in October 1990 for the entire sections. Positive transport is into the box (south at 5°30'S, west at 33°W and north at 9°S)*

Depth layer	VM-ADCP	Geostrophy
(a) 5°30'S		
0–100 m	−1.8	−1.2
0–200 m	−8.1	−7.9
(b) 33°W		
0–100 m	1.1	*
0–200 m	4.2	*
(c) 9°S		
0–100 m	3.8	*
0–200 m	10.7	*

*no CTDs available

computations. As can be seen from Table 2 the adjustment of the geostrophic computation at 5°30'S leads to only a small increase in transport in the upper 1000 m from 20.2 Sv without adjustment to 22.5 Sv with adjustment. The net flow after adjustment is 19.5 Sv when the Ekman flow of 3 Sv is included compared to 19.6 Sv from the IADCP.

At 10°S the lowered ADCP at two eastern stations showed an unrealistic velocity increase below 500 m depth which was not observed in the geostrophic profiles. The station distance was also large and might have caused aliasing problems. Because of this discrepancy the IADCP transport for the layer 0–1000 m in Table 2 is given in brackets and includes only the transport from the shelf out to the flow reversal below 500 m depth. As no Pegasus profiles are available at 10°S, and due to the inconsistencies in two of the deeper IADCP profiles, no adjustment could be made for the 10°S section. The IADCP profiles within the area of the NBUC indicate a low velocity layer near 1150 m depth. Together with the good resemblance of the geostrophic plus Ekman transport with the direct transport in the upper 250 m (Table 2c), the reference of $\sigma_1 = 32.15$ kg m^{-3} should also be appropriate at 10°S.

A different result was found for the diagonal section connecting the 5°30'S and the 10°S sections where the station spacing was 1° latitude. LADCP velocities along this section were fairly weak, showing no coherent structures from one station to the next. This indicates that the station grid was inadequate to resolve the flow structures, and transport estimates from the IADCP had to be regarded as meaningless. As the direct measurements
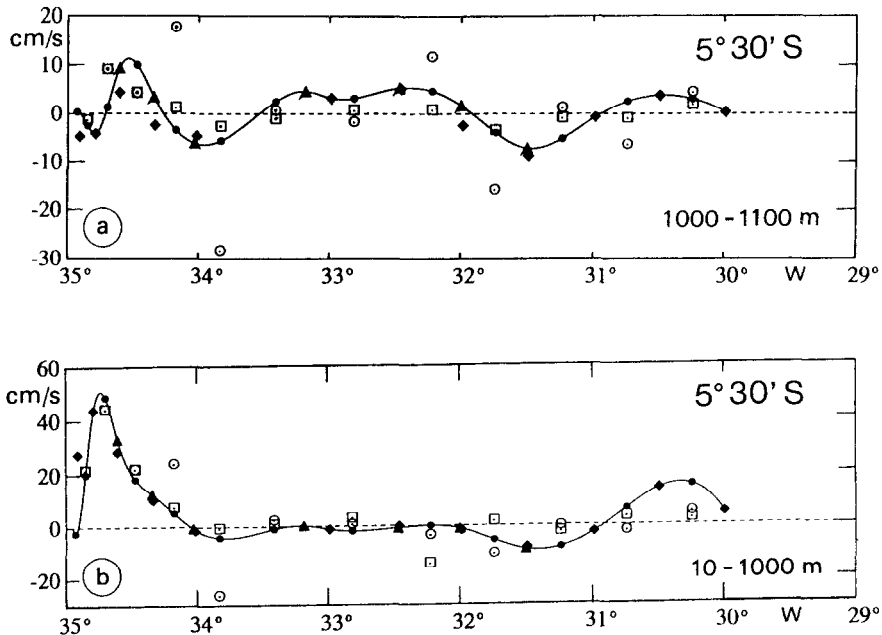

Fig. 9. Mean velocity for the layer (a) 1000–1100 m depth and (b) 10–1000 m depth at 5°30'S in November 1992 from the IADCP measurements (solid diamonds), from Pegasus profiles (solid triangles), the geostrophic computation relative to the density $\sigma_1 = 32.15$ kg m^{-3} (open squares) and relative to the density $\sigma_4 = 45.90$ kg m^{-3} (open circles). Solid dots on the curve indicate the location of the spline-fitted curve through Pegasus and IADCP mean velocities in the middle of a station pair, where the geostrophic velocity profile is centered.

contain no information on the flow field inbetween, a computation of transports from the lADCP would result in a random number and would not be based on physics. The transport has to be taken from the geostrophy, but the transport without adjustment led to an inflow into the box which is not required to balance the transports found at 5°30'S and 10°S and which is inconsistent with the upper ocean currents measured by the VM-ADCP. Although the lADCP resolution was not adequate for transport calculations, it can provide some information regarding the reference layer. The depth of about 1150 m, typical for the reference $\sigma_1 = 32.15$ kg m^{-3}, showed relatively large velocities, while at a depth of about 500 m all lADCP profiles indicated low velocities. Therefore, an adjustment was made for the diagonal section to the lADCP fitted cubic curve through the mean velocity between 400 and 700 m depth. The adjusted transport (Table 2) for the upper 1000 m was an outflow of 0.9 Sv compared to an inflow of 6.6 Sv into the box without the adjustment. This result might be an indication that for the diagonal section the reference of $\sigma_1 = 32.15$ kg m^{-3} is not adequate. It has to be mentioned that a different choice of the layer for the adjustment, such as 500–700 m, leads to transport differences of up to 2.5 Sv, which has to be regarded as a typical error for the adjustment at the diagonal section. Normally it is expected that at a reference level both velocity components become small. Of course in some regions one component might vanish while the other does not. This is the case at about 31°W where the meridional flow was small while the zonal flow was not, as can be seen from the direct velocity observations.

As discussed before, the density of $\sigma_1 = 32.15$ kg m^{-3} as reference depth seems appropriate for the two zonal sections, and a major difference in transport is found for the diagonal section between the geostrophic flow and the geostrophic flow adjusted to the ADCP. If the transport for the adjusted flow for the diagonal section is combined with the geostrophic flow of the zonal sections (Table 2), the 0–1000 m imbalance is reduced from 6.3 Sv to −1.2 Sv for geostrophy and to 1.2 Sv if the Ekman flow is added. This imbalance is lower than the error of 2.5 Sv associated with the choice of the layer of adjustment.

DISCUSSION

Comparison to historical data

The flow field in a closed box off the coast of Brazil in the source region of the NBC was investigated using different observational methods for austral spring in November 1992 and October 1990. The observations showed a strong North Brazil Undercurrent with transports of more than 22 Sv in the upper 1000 m in the latitude range 5°S–10°S. In an evaluation of historical data, Stramma et al. (1990) found a much weaker northward flow of about 5 Sv at 8°S–9°S in February and March from geostrophic computations relative to a density $\sigma_0 = 27.05$ kg m^{-3}. This density layer was used for the zonal sections and represents the boundary between the Subantarctic Central Water (SACW) and the Antarctic Intermediate Water (AAIW) at depth of about 360–670 m. This layer was appropriate in the Brazil Current region, where Pegasus measurements (Evans and Signorini, 1985) showed the current reversal between the southward Brazil Current and the northward spreading AAIW. In the NBUC region, however, the flow of the NBUC as well as the flow of the AAIW are to the north. Therefore, this density layer used by Stramma et al. (1990), who had no direct velocity observations available, was not appropriate to estimate the total northward transport of the NBUC. This is clearly

illustrated by Fig. 4b, which shows that the depth of the density $\sigma_0 = 27.05$ kg m^{-3} lies in a region of intense northward currents.

According to these findings the transports were recalculated for the zonal sections (except the two *Meteor* sections from 1926) north of 16°S used by Stramma *et al.* (1990) relative to the density of $\sigma_1 = 32.15$ kg m^{-3}. In all cases there was a northward transport near the coast with much higher transports compared to the reference used by Stramma *et al.* (1990). Hence, also from the historical data base, the NBUC can be described as a western boundary current north of 16°S, providing the appropriate reference layer is used. Compared to the transports in austral spring (this investigation), the transports from the historical data base, all taken in austral fall, showed smaller transports. None of the fall sections showed NBUC transports larger than 19 Sv for the layer 0–1000 m. These sections indicated a seasonal cycle between 3 Sv and 10 Sv. The only section available to Stramma *et al.* (1990), from the month October at 7°05'S by R.V. *A. Saldanha*, had some data problems not noticed before and could not be used. The effect of the two reference layers is illustrated by the R.V. *Atlantis* section at 12°15'S. Using $\sigma_0 = 27.05$ kg m^{-3} Stramma *et al.* (1990) obtained 2.2 Sv southward transport (0–500 m), whereas with the deep reference the transport was 10.2 Sv northward. The total 0–1000 m layer transport was 14.3 Sv. For a cross-check, the *Meteor* transport at 10°S in November 1992 was computed relative to $\sigma_0 = 27.05$ kg m^{-3}. From the coast to the flow reversal, the 0–500 m transport was reduced from 16.0 Sv to 2.3 Sv and for 0–1000 m from 22.2 to 1.1 Sv. Summarizing, estimates of the NBUC transports depend strongly on the choice of the appropriate reference layer. Here it is shown that a shallow reference led to incorrect transports suggesting the source of the NBUC further north.

Seasonal signal

The recalculated transports based on sections from the historical data base of the World Oceanographic Data Center indicate seasonal variability of the NBUC near 10°S. Larger transports were found in austral spring and smaller values in austral fall. This is in agreement with the evaluation of the WOCE–CME (world ocean circulation experiment–community modeling effort) model by Schott and Böning (1991). In their Fig. 9 the transports within the upper 519 m at 5°S between 30°W and the coast are 13.2 Sv on average with the extrema of 20.9 Sv in August and 8.9 Sv in February. This is in contrast to the maps by Cochrane *et al.* (1979), where the NBC appears stronger in February–April and weaker in July–September.

A CTD section was made along 5°30'S in June 1991 from R.V. *Meteor* during cruise M16-3. The section of June 1991 showed the same clear subsurface velocity core at 5°S, and the undercurrent is a feature of the entire year and not restricted to a part of the year. The transport computed consistently with the other sections of the upper 1000 m west of the flow reversal was 34.2 Sv and therefore larger than the transports observed in October 1990 and November 1992. The larger transport for June 1991 was also present in transport estimates from the Pegasus system (U. Send, pers. com.), i.e. not dependent on the choice of a reference layer. The VM-ADCP showed a 0–250 m transport across the entire 5°30'S section of 16 Sv in June 1991, which is also larger than for the two other *Meteor* realizations reported here of about 8 Sv (Tables 2 and 3). This finding is consistent with the model result, as the June section is closer to the maximum in August in the CME-model than the October 1990 and November 1992 section. The sections from the historical data set in

February and March correspond to the minimum transport in February. However, further north at the equator Schott *et al.* (1993) found only a small seasonal cycle of ± 3 Sv in the upper 600 m superimposed on 30.5 Sv annual mean NBC transport. Their calculations based on moored current meter data and ship observations showed the transport maximum in June–August and minimum in northern spring. Therefore, the seasonal signal observed in the "source region of the NBC" seems to be present at the equator, although reduced in magnitude, while the mean transport of the upper 600 m is much larger at the equator than further south. At the equator a spectral decomposition of the intraseasonal scale variance of the mooring data shows energy maxima at two different periods of about one and two months (Schott *et al.*, 1993). No evidence was found in the literature as to whether these variabilities exist also at 5°30'S–10°S, but if they do they might influence the amplitude of the seasonal signal as estimated from the sections used.

Final remarks

In November 1992 there was almost no westward flow at 30°W between 10°S and 5°30'S. Therefore, the branch of the South Equatorial Current which feeds the NBUC had to be located south of 10°S, while additional inflow into the NBC, mainly near the surface, might come from a branch of the SEC north of 5°S. From the data represented here and the re-evaluated sections from the historical data base, it was shown that the NBUC is a permanent feature of the circulation north of 10°S and that the origin must be further south. With the weak signal at the sea surface, or even a reversed southward surface flow observed in ship drifts and surface drifters, and with no direct current observations available, the NBUC was difficult to detect, as the major velocities are located in a strong subsurface core.

The formation of the NBUC south of 10°S is also present in the WOCE-CME model (Schott and Böning, 1991), where the flow is fed by zonal inflow in the latitude range 11°–13°S. These model results were forced to the seasonally varying Levitus (1982) climatology, and the model domain covered the Atlantic between 65°N and 15°S; therefore the results might be influenced by the boundary conditions at the southern boundary. Nevertheless, the WOCE-CME model describes a NBUC similar to our observations. In a simple model with selected combinations of different basin geometries, wind-stress fields and thermohaline forcing pattern, Onken (1994) described the asymmetries of the western boundary current in the entire Atlantic. Between 8°S and 20°S the model results differed considerably from the observations of Stramma *et al.* (1990). At 10°S the model required a northward transport of about 21 Sv, and our present observations are in good agreement with the model result.

The NBUC was observed with a subsurface core at about 200 m depth at 5°30'S and 10°S. Such a subsurface flow, was, to the authors knowledge, not described before from velocity observations, but was proposed by Schott and Böning (1991) evaluating the WOCE-CME model. Defant (1936) discussed the distribution of the salinity maximum at 100–150 m depth as a southern hemispheric undercurrent along the coast of South America. The subsurface salinity maximum was observed already on a section at about 6°S (Stephan 1911 section, Defant 1936) described by Merz (1912).

On a section at 35°W, off Brazil, carried out in November 1992 during *Meteor* cruise 22 with Pegasus profilers and lADCP, a subsurface core was observed for the NBUC, while the velocity maximum in some instances moves up to the surface before reaching the

equator at 44°W, where the maximum velocity was observed at the surface (Schott *et al.*, 1993). One possible reason for the reduced surface flow between 5°30'S and 10°S could be the southward component of the Ekman transport. Rough estimates of the Ekman surface velocity with equations given in Pond and Pickard (1978) led to velocities of about 30 cm s^{-1} at 5°30'S as well as at 10°S but with an Ekman depth which was 103 m at 5°30'S and 64 m at 10°S for the November mean wind stress. This Ekman velocity would lead to a considerable reduction of the near surface flow field. However, the observed shear in the near surface layer was larger than indicated by an Ekman flow of such magnitude.

At about 150 m depth at 5°30'S the northward flow, with velocities of more than 10 cm s^{-1}, extends as a velocity tongue about 70 km further to the east than the surrounding velocity field. This feature was present in all observations at 5°30'S, but not at 10°S. The reason for this feature remains an open question. One possible explanation is that the eastern part of the subsurface core contributes to the South Equatorial Undercurrent.

For the two zonal lADCP sections the velocity profiles were correlated from one station to the next, and within the error bounds the transports were the same as for geostrophic calculations. However, the direct current observations were very helpful to determine the appropriate reference layer. They clearly showed that $\sigma_1 = 32.15$ kg m^{-3} was preferable compared to $\sigma_4 = 45.90$ kg m^{-3}, which was superior for the deep flow (Rhein *et al.*, 1995). Although the section-wide transport was about the same for both reference layers, the details were not. In particular the width and transport of the NBUC would have been overestimated by about 20 km and 5 Sv, respectively, with the deep reference. Furthermore, the direct observations might serve as a reference (level of known motion). For the chosen reference layer (1000–1100 m depth) the overall effect was small with the adjusted geostrophic transports at 5°30'S about 10% larger than from geostrophy alone ($\sigma_1 = 32.15$ kg m^{-3}). A larger effect (with larger uncertainties) was found at the diagonal section where the adjusted transport strongly reduced the imbalance of the box transport.

REFERENCES

Arnault S. (1987) Tropical Atlantic geostrophic currents and ship drifts. *Journal of Geophysical Research*, **92**, 5076–5088.

Cochrane J. D., F. J. Kelly Jr and C. R. Olling (1979) Subthermocline countercurrents in the western equatorial Atlantic Ocean. *Journal of Physical Oceanography*, **9**, 724–738.

Defant A. (1936) *Stratification and circulation of the Atlantic Ocean: The troposphere*, translated by W. J. Emery (1981) Amerind Publishing Co, New Dehli, 113 pp.

Evans D. L. and S. S. Signorini (1985) Vertical structure of the Brazil Current. *Nature*, **315**, 48–50.

Fischer J. and M. Visbeck (1993) Deep velocity profiling with self-contained ADCP's. *Journal of Atmospheric and Oceanic Technology*, **10**, 764–773.

Levitus S. (1982) Climatological Atlas of the World Ocean, NOAA Professional paper 13, 173 pp.

Merz A. (1912) Eine ozeanographische Forschungsreise im Atlantischen Ozean. *Verhandlungen des XVIII Deutschen Geographentages zu Innsbruck* 1912, Berlin 1912, 82–90.

Molinari R. L. (1982) Observations of eastward currents in the tropical South Atlantic Ocean: 1978–1980. *Journal of Geophysical Research*, **87**, 9707–9714.

Molinari R. L. (1983) Observations of near-surface currents and temperature in the central and western tropical Atlantic Ocean. *Journal of Geophysical Research*, **88**, 4433–4438.

Molinari R. L., R. A. Fine and E. Johns (1992) The deep western boundary current in the western tropical North Atlantic Ocean. *Deep-Sea Research*, **39**, 1967–1984.

Onken R. (1994) The asymmetry of Western Boundary Currents in the upper Atlantic Ocean. *Journal of Physical Oceanography*, **24**, 928–948.

Pond S. and G. L. Pickard (1978) *Introductory dynamic oceanography*, Pergamon Press, Oxford, 241 pp.

Reid J. L. (1989) On the total geostrophic circulation of the South Atlantic Ocean: Flow patterns, tracers and transports. *Progress in Oceanography*, **33**, 1–92.

Reid J. L. (1994) On the total geostrophic circulation of the North Atlantic Ocean: Flow patterns, tracers and transports. *Progress in Oceanography*, **23**, 149–244.

Rennell J. (1832) *An investigation of the currents of the Atlantic Ocean, and of those which prevail between the Indian Ocean and the Atlantic*. J. G. & F. Rivington, London, 299 pp, 2 plates.

Reverdin G. and M. J. McPhaden (1986) Near-surface current and temperature variability observed in the equatorial Atlantic from drifting buoys. *Journal of Geophysical Research*, **91**, 6569–6581.

Rhein M., L. Stramma and U. Send (1995) The Atlantic Deep Western Boundary Current: Water masses and transports near the equator. *Journal of Geophysical Research*, **100**, 2441—2457.

Richardson P. L., G. E. Hufford, R. Limeburger and W. S. Brown (1994) North Brazil Current retroflection eddies. *Journal of Geophysical Research*, **99**, 5081–5093.

Richardson P. L. and D. Walsh (1986) Mapping climatological seasonal variations of surface currents in the tropical Atlantic using ship drifts. *Journal of Geophysical Research*, **91**, 10537–10550.

Schott F. and C. W. Böning (1991) The WOCE model in the western equatorial Atlantic: upper-layer circulation. *Journal of Geophysical Research*, **96**, 6993–7004.

Schott F., J. Fischer, J. Reppin and U. Send (1993) On mean and seasonal currents and transports at the western boundary of the equatorial Atlantic. *Journal of Geophysical Research*, **98**, 14353–14368.

Send U. (1994) The accuracy of current profile measurements-effect of tropical and mid latitude internal waves. *Journal of Geophysical Research*, **99**, 16229–16236.

Servain J. and S. Lukas (1991) Climatic Atlas of the tropical Atlantic wind stress and sea surface temperature. IFREMER report, 133 pp.

Spain P. F., D. L. Dorson and H. T. Rossby (1981) PEGASUS: A simple acoustically tracked velocity profiler. *Deep-Sea Research*, **28**, 1553–1567.

Stramma L. (1991) Geostrophic transport of the South Equatorial Current in the Atlantic. *Journal of Marine Research*, **49**, 281–294.

Stramma L., Y. Ikeda and R. G. Peterson (1990) Geostrophic transport in the Brazil Current region north of 20°S. *Deep-Sea Research*, **37**, 1875–1886.

Stramma L. and H. J. Isemer (1988) Seasonal variability of meridional temperature fluxes in the eastern North Atlantic Ocean. *Deep-Sea Research*, **46**, 281–299.